Electronic Supplementary Information

Stimuli-Responsive Spin Crossover Nanoparticles for Drug Delivery and DNA-Binding Studies

Christina D. Polyzou,*[,a] Patroula Gkolfi,[a] Christos T. Chasapis,[b] Vlasoula Bekiari,[c] Ariadni Zianna,[d] George Psomas,[d] Malina Ondrej[e] and Vassilis Tangoulis*[,a]

a. Department of Chemistry, Laboratory of Inorganic Chemistry, University of Patras, 26504 Patras, Greece. E-mail: chpolyzou@upatras.gr, vtango@upatras.gr

b. NMR Facility, Instrumental Analysis Laboratory, School of Natural Sciences, University of Patras, 26504 Patras, Greece.

c. Department of Crop Science, University of Patras, 30200 Messolonghi, Greece.

d. Laboratory of Inorganic Chemistry, Department of Chemistry, Aristotle University of Thessaloniki, Thessaloniki GR-54124, Greece.

e. Regional Centre of Advanced Technologies and Materials, Czech Advanced Technology and Research Institute (CATRIN), Palacký University Olomouc, Czech Republic.

MATERIALS

PHYSICAL MEASUREMENTS

- *FT-Infrared Spectroscopy*
- *UV-Vis Spectroscopy*
- *Drug Release Study*
- *Drug Loading*
- *Magnetic Study*
- *Zeta-Potential Study*
- *HR-TEM Microscopy*
- *DNA–binding Studies*

Materials

All manipulations were performed under aerobic conditions using reagents and solvents as received. The reagents (S)-Naproxen (NAP), 1-ethyl-3-(3-dimethylaminopropyl)carbodiimide (EDC) and 1-hydroxybenzotriazole (HOBt) were purchased from Sigma Aldrich.

Synthesis of 1@NAP

Direct Coupling of NAP on doped AmNPs **1**: The synthesis of doped AmNPs **1** has been described previously in detail.[32] Direct Coupling of NAP on doped NPs **1** (**1@NAP**): 20 mg of doped NPs **1** were sonicated for 15 min in 10 mL CH_2Cl_2. Then NAP (7.5 mg), EDC (6.33 mg) and HOBt (8.92 mg) were added in the suspension and vigorous stirring was followed for 24 h. The resulting mixture of NPs-NSAIDs and unreacted excess of the coupling agents (EDC and HOBt) was initially isolated through centrifugation at 6000 rpm. Then after three washing cycles with CH_2Cl_2 (8 mL) resulted in pure NPs-NSAIDs which finally dried under vacuum.

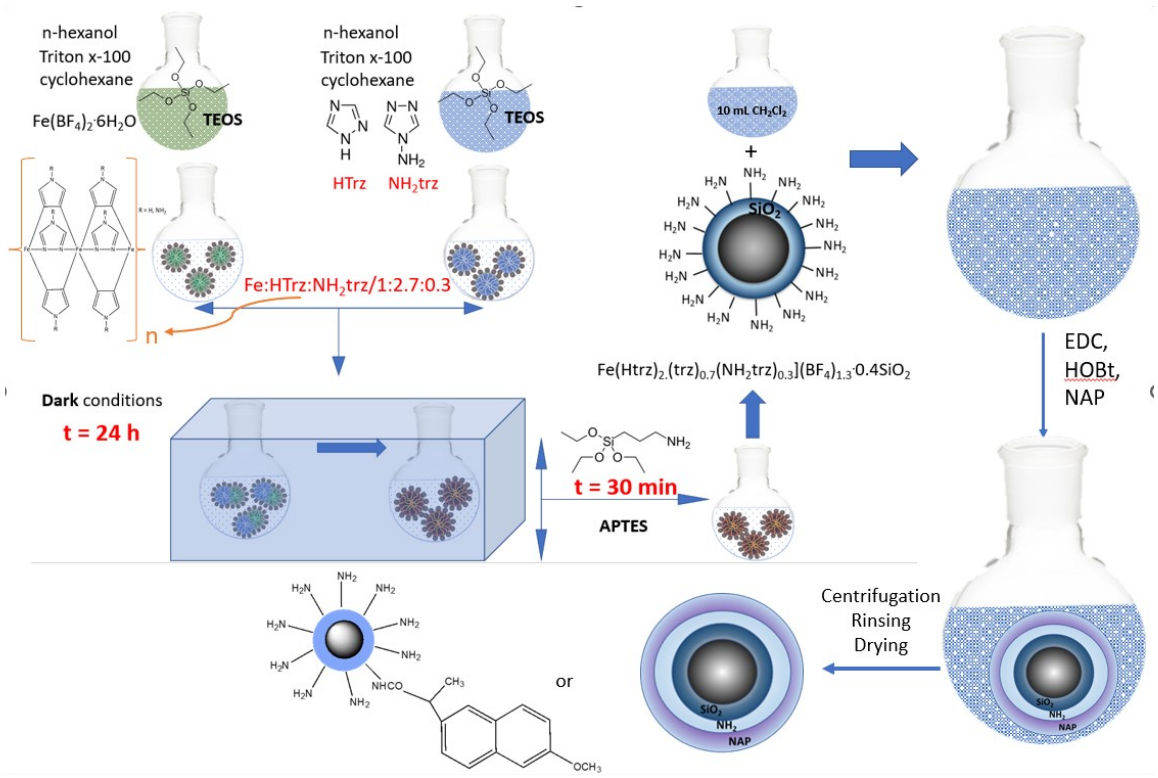

Fig. S1. Synthetic strategy for the preparation of **AmNPs 1** and **1@NAP**.

Physical Measurements

IR spectra (4000-400 cm^{-1}) were recorded using a Perkin-Elmer 16PC FT-IR spectrometer with samples prepared as KBr pellets. UV-Vis absorption spectra were recorded between 280 and 1100 nm by using the spectrometer PGS-2 produced by Carl Zeiss. TEM study performed utilizing a FEI CM20 TEM operating at 200 kV. TEM specimens prepared by drop casting a 3 µL droplet of nanoparticles suspension in acetone on a carbon coated Cu TEM grid. The size of the particles determined by ‘‘manual counting’’ using ImageJ software (https://imagej.net). The direct-current (DC) magnetic susceptibility measurements were measured on powder samples using a physical-properties measurement system (PPMS, Quantum Design) at 2 – 300 K with a rate of 1 K min^{-1} under an applied dc magnetic field of 1000 Oe. The experimental data were corrected for the diamagnetism and signal of the sample holder and the Pascal constants were used for the diamagnetic corrections. The emission characterization of 1@NAP was recorded on a Cary Eclipse emission spectrophotometer. The NMR spectra were recorded with a Bruker Ascend 600 spectrometer operating at a ^{1}H Larmor frequency of 600.13 MHz. All the proton one-dimensional NMR experiments were selected using the subsequent acquisition parameters: 32 scans, a spectral width of 10.822 Hz and relaxation delay of 2 s. The spectra were collected at the 298.15 K temperature. Spectra were manually corrected for phase and baseline distortions using TopSpin 3.6 (Bruker BioSpin srl).

FT-Infrared Spectroscopy

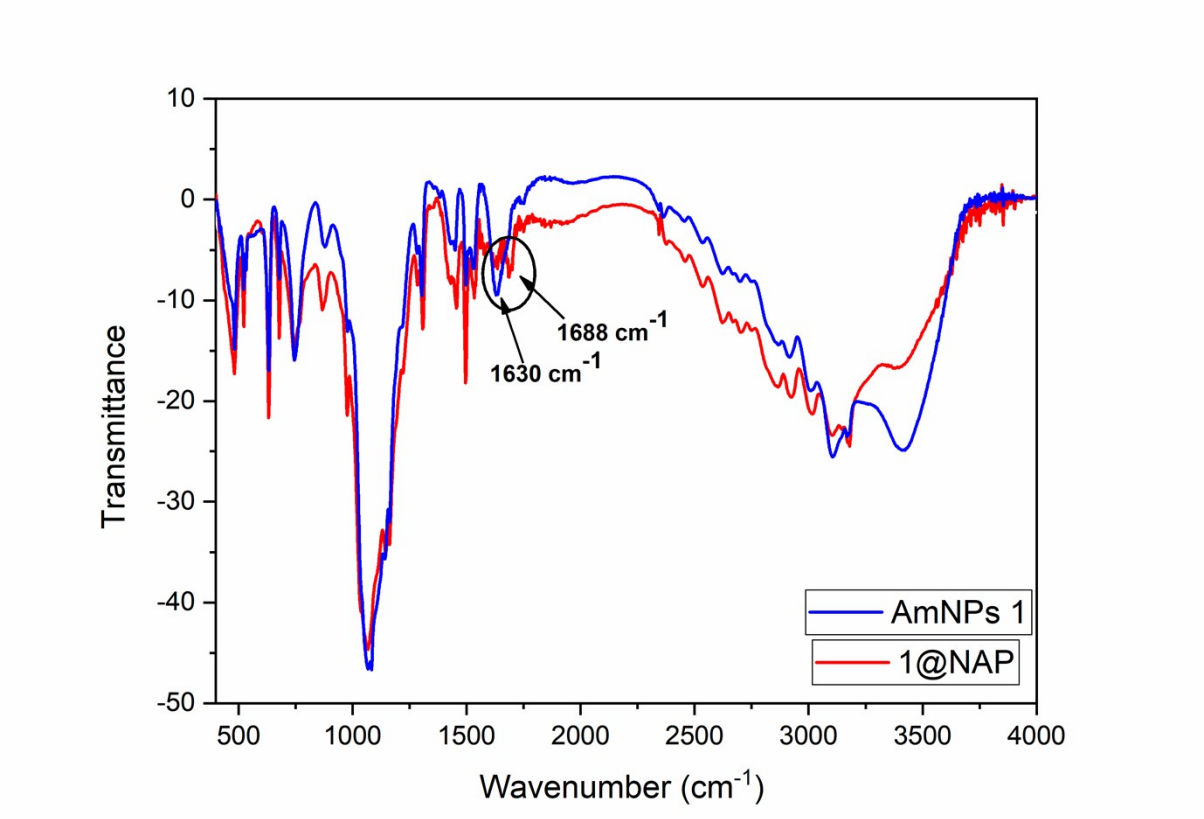

Fig. S2. FT-IR spectra of **AmNPs 1** and **1@NAP**.

UV-Vis Spectroscopy

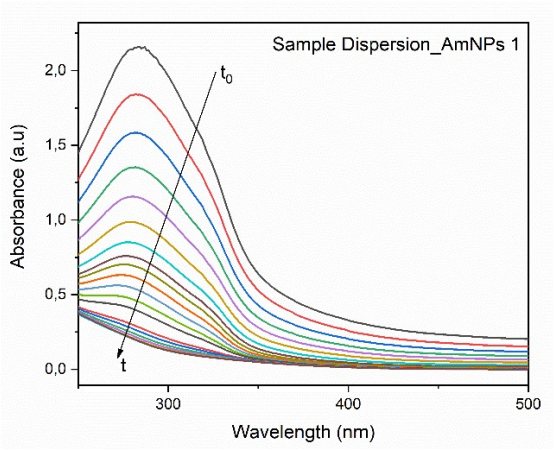

(A)

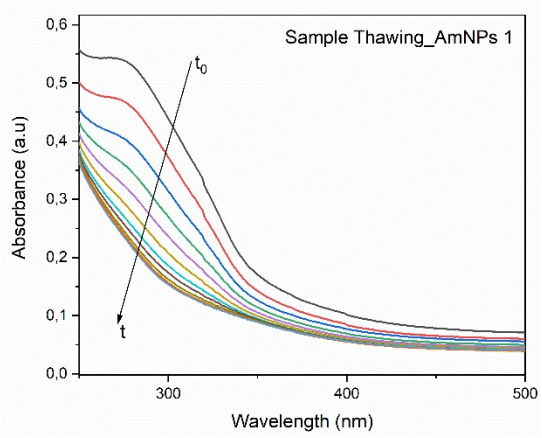

(B)

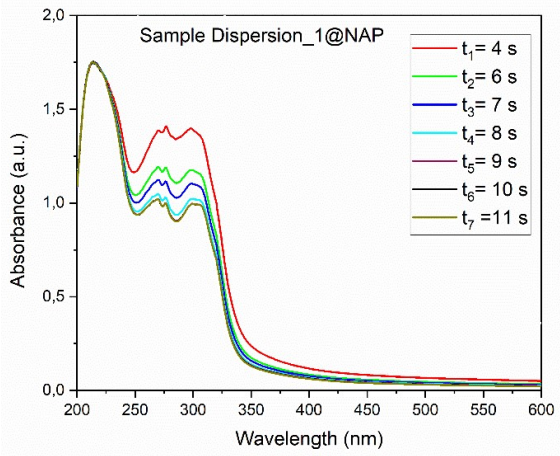

(C)

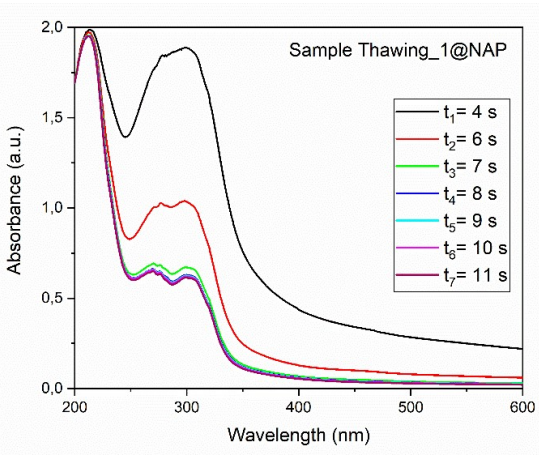

(D)

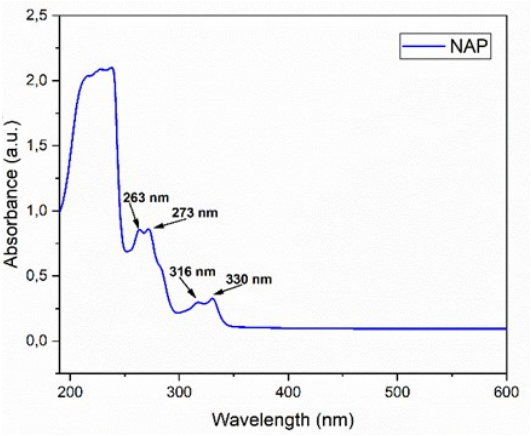

(E)

Fig. S3. Time-dependent UV-vis spectrum of **AmNPs 1** (A) and **1@NAP** (C), respectively, immediately after their dispersion in H_2O. Time-dependent UV-vis spectrum of **AmNPs 1** (B)

and **1@NAP** (D), respectively, during sample thawing from -20 ^{o}C to RT. UV-Vis spectrum of **NAP** (E).

In the case of **AmNPs 1**, the absorption band around 280 nm -corresponding to an MLCT transition- showed a drastic reduction of its intensity as the samples switched from the LS to HS state of Fe^{II} accompanied by a color change in the dispersion from violet to colorless (Fig. S3A). In the case of **1@NAP**, the related absorption band (~280 nm) is also resolved along with the characteristic bands of the NAP (263 and 273 nm) (Fig. S3C). An analogous reduction of its intensity is presented denoting that the Fe^{II} preserves its SCO characteristics while the dispersion of **1@NAP** is accompanied by a color change from violet to colorless. It should be mentioned here that apart from the MLCT absorption band, the NAP related bands (Fig. S3E) in the area 260-330 nm are also observed in the spectrum. After the completion of the transition from LS-HS the spectrum of the **1@NAP** presents solely the time-independent absorption bands of the NAP. The SCO phenomenon is considered reversible for **AmNPs 1** since the color can change from colorless to violet using a cooling process according to which we observe the reappearance of the MLCT absorption at 280 nm denoting that the LS state is now fully occupied. Further heating of the sample back to RT provides a new change of the color from violet to colorless, accompanied by the disappearance of the MLCT absorption peak due to a new spin transition from LS to HS state (Fig. S3B). Following the same heating-cooling protocol described before for the **AmNPs 1**, we also confirmed that the SCO phenomenon of the **1@NAP** is retained in aqueous solution (Fig S3D).

Drug release study

Drug release behavior was investigated according to the following procedure: 1 mg of the studied material was dispersed in 5 mL of two buffered solutions (pH = 4.1 and 6.8) under stirring at room temperature. At predetermined time intervals the solution was transferred in a cuvette and the emission intensity of NAP at 360 nm under excitation at 230 nm was recorded.

Cumulative release (%) was expressed as:

$$\textit{Cumulative release (\%)} = \frac{W_t}{W_{drug}} \times 100 \quad (1)$$

where W_t and W_{drug} indicate the weight of drug released from the hybrid material at time t, and the total amount of loaded drug, respectively. W_t and W_{drug} were calculated from the calibration curve of free naproxene emission intensity at various concentrations, under the same excitation and emission wavelengths.

Drug Loading

From the calibration curve of the emission intensity of NAP at 354 nm the percentage of the drug loading can also be calculated as: 1 mg of the loaded material was dispersed in 5 mL of buffer solution giving 0.2 mg/mL final concentration. In this dispersion the maximun emission intensity of NAP under the same measurement conditions (excitation and emission monochromator slits) was 852 (a.u.). From the equation of the calibration curve of NAP in PBS buffer (pH 6) the concentration of NAP in this dispersion is calculated at 0.1 mg/mL. As this value corresponds to 0,2 mg/mL of the studied loaded material, the loading is calculated at 500 mg/g (50%).

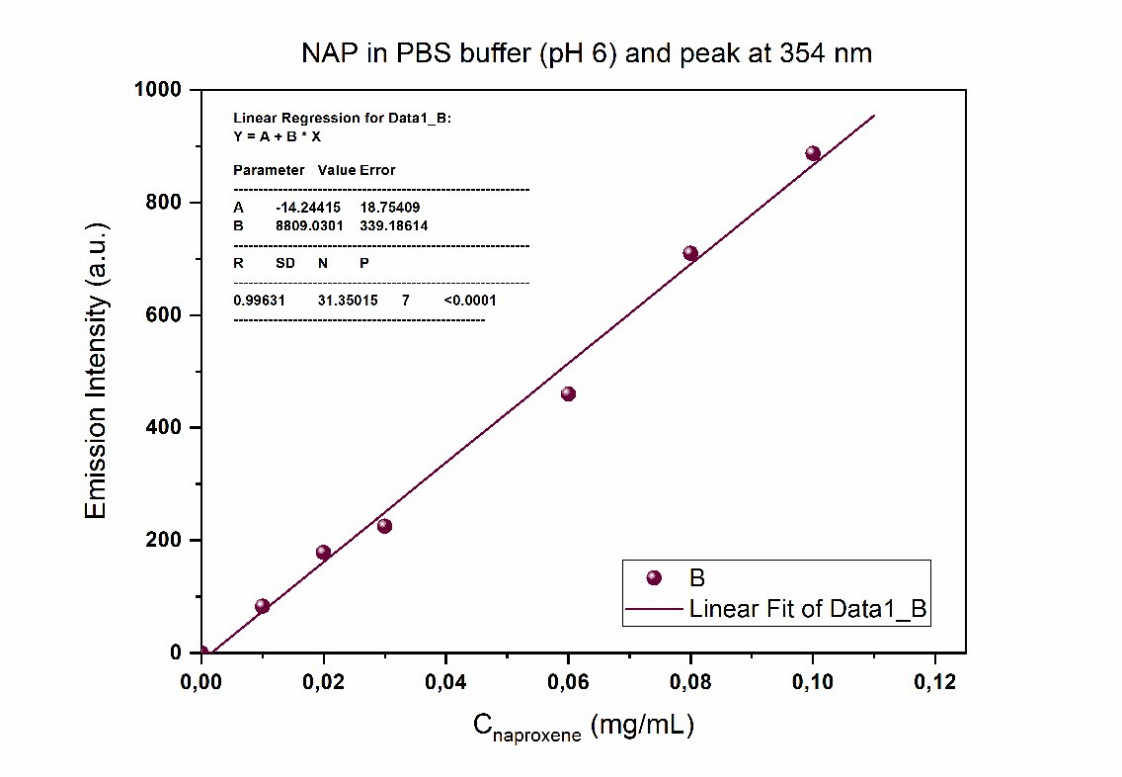

Fig. S4. Calibration curve of **NAP** in PBS buffer (pH 6).

Calculation of NAP loading percentage:

The absorbance of NAP at 354 nm is equal to 852. According to this Y= -14,24415 + 8809,0301*X => X=Y+14,24415/8809,0301. When Y=852 => X= 0.1 mg/mL of NAP.

In the dispersion of 5 mL was initially dissolved 1 mg of 1@NAP, so in a dispersion of 1 mL was finally dissolved 0.1 mg of 1@NAP. In 0.2 mg of 1@NAP there are 0.1 mg of NAP, so in 100 mg of 1@NAP there are finally 50 mg of NAP. Thus, the loading precentage is estimated at around 50%. Below there is the evolution of emission spectra of NAP with increasing concentrations.

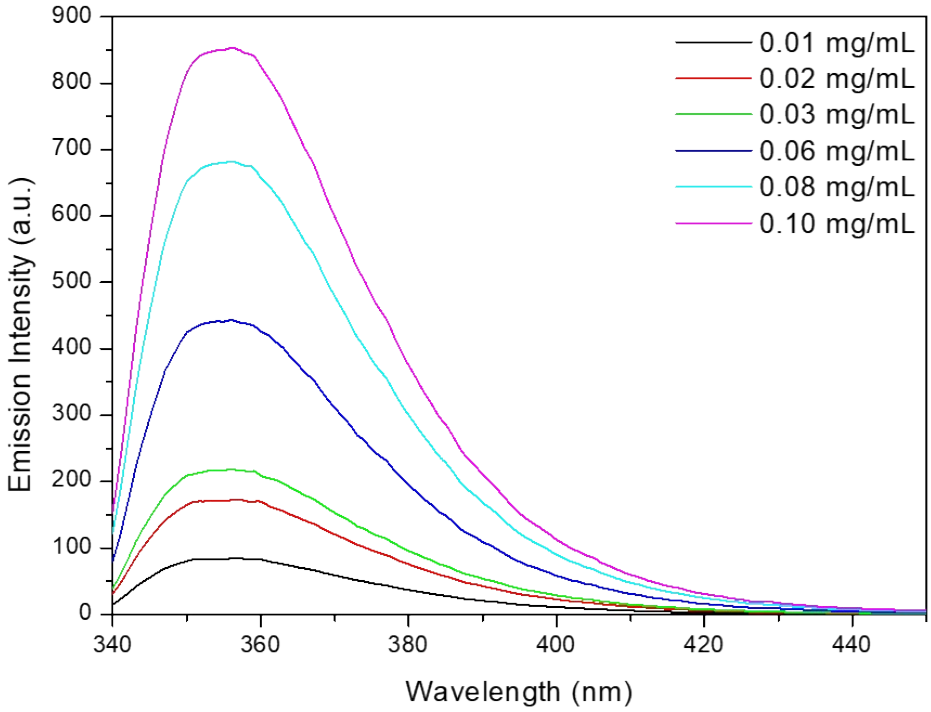

Fig. S5. Emission spectrum of **NAP** in different concentrations.

Magnetic Study

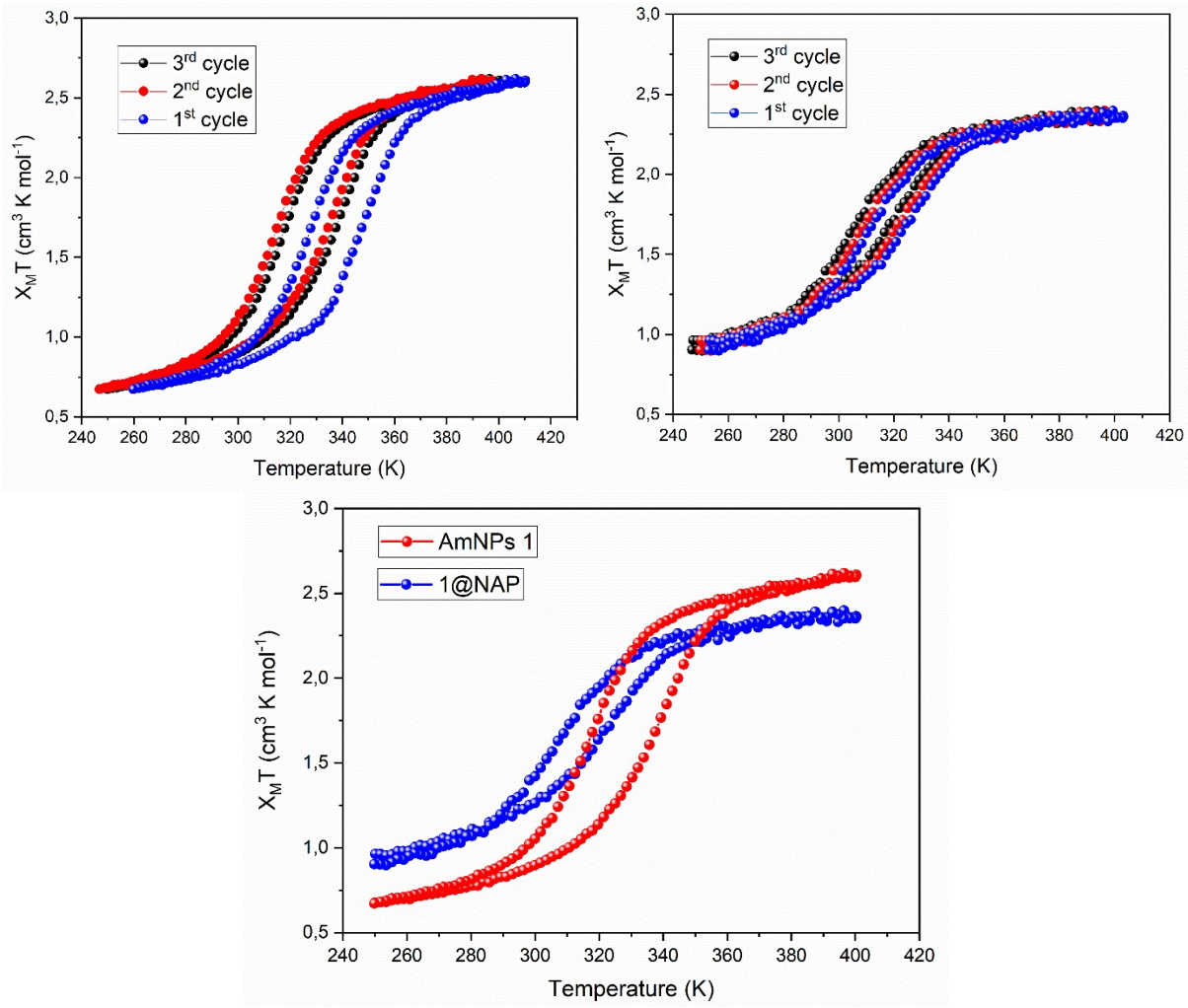

Fig. S6. Three cycles of thermal dependence of the $\chi_M T$ product for **AmNPs 1** with a rate of K 1 min^{-1} (left/up). Three cycles of thermal dependence of the $\chi_M T$ product for **1@NAP** with a rate of K 1 min^{-1} (right/up). Comparison of the thermal dependence of the $\chi_M T$ product between **AmNPs 1** and **1@NAP** with a rate of K 1 min^{-1} (2^{nd} cycle, down).

Table S1. Magnetic parameters derived from thermal susceptibility measurements of the AmNPs 1 and 1@NAP.

Compound	T_{incr} ↑(K)	T_{decr} ↓(K)	ΔT	$X_M T$ (cm^3 K mol^{-1})
AmNPs 1	338	318	20	2.60
1@NAP	321	309	12	2.36

Zeta-potential Study

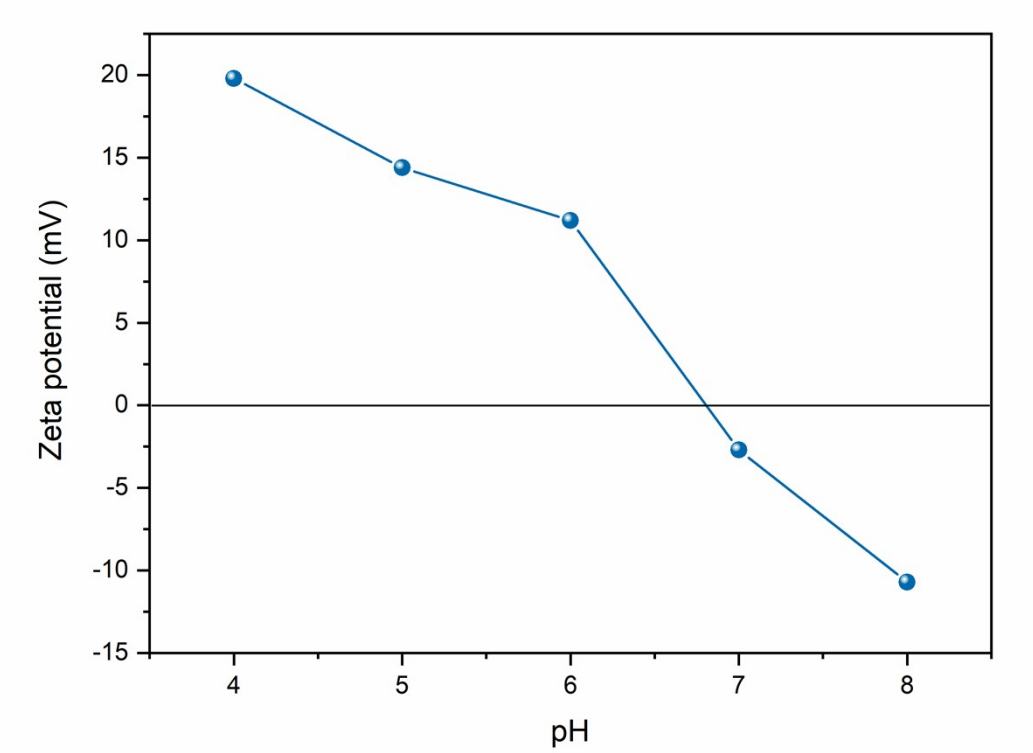

Fig. S7. Zeta potential as a function of pH for **1@NAP**.

HR-TEM Microscopy

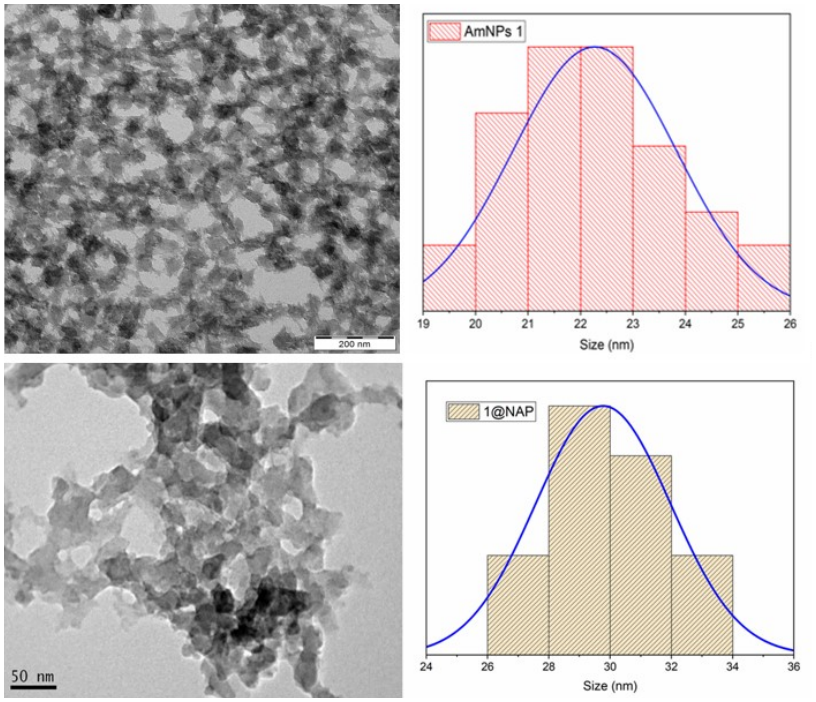

Fig. S8. TEM images and size distribution for **AmNPs 1** (up) and **1@NAP** (down).

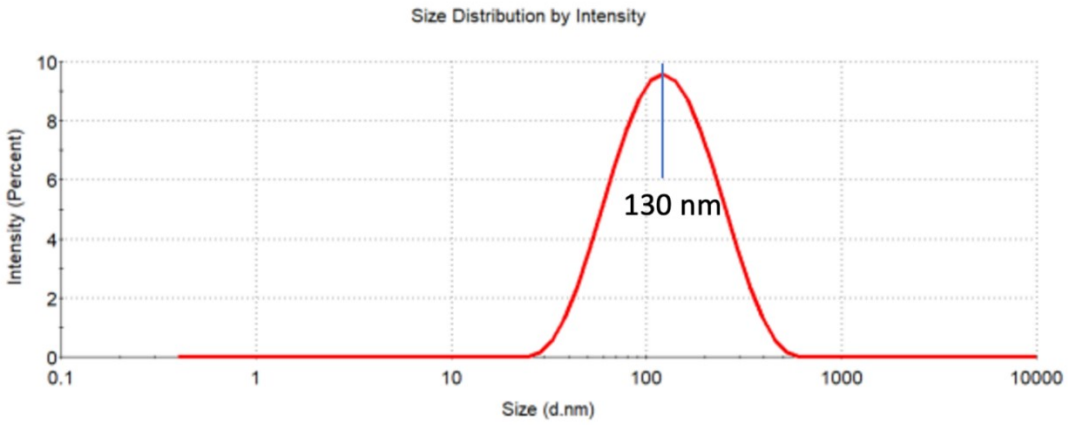

Fig. S9. DLS measurements for **1@NAP** in aqueous dispersion.

DNA–binding studies

The interaction of compound **1@NAP** with CT–DNA was investigated by UV–vis spectroscopy, viscosity measurements and fluorescence emission spectroscopy studies.

Binding study with CT DNA by UV–vis spectroscopy: UV–vis spectroscopy was used for the evaluation of the interaction of the compound with CT DNA, and specifically the possible binding mode of the compound to CT DNA. Control experiments with DMSO were performed and no changes in the spectra of CT DNA were observed.

In order to determine the binding mode, the UV–vis spectra of **1@NAP** were recorded for a constant concentration with increasing concentrations of CT DNA for diverse *r* values (*r* = [complex]/[DNA]). Effective use of the changes in the absorbance at the corresponding λ_{max} of the UV–vis spectra was made and the DNA–binding constants (K_b, in M^{-1}) of the compounds were calculated by the Wolfe–Shimer equation (eq. S1)[S1] and the plots [DNA]/(ε_A–ε_f) *versus* [DNA]:

$$\frac{[DNA]}{(\varepsilon_A - \varepsilon_f)} = \frac{[DNA]}{(\varepsilon_b - \varepsilon_f)} + \frac{1}{K_b(\varepsilon_b - \varepsilon_f)} \qquad \text{(eq. S1)}$$

where [DNA] = the concentration of DNA in base pairs, ε_f= the extinction coefficient for the free compound at the corresponding λ_{max}, $\varepsilon_A = A_{obsd}/[compound]$ and ε_b= the extinction coefficient for the compound in the fully bound form. K_b is given by the ratio of slope to the y intercept in plots [DNA]/(ε_A–ε_f) *versus* [DNA].

CT DNA–binding studies by viscosity measurements: The viscosity of DNA (0.1 mM) in buffer solution was measured in the absence and presence of increasing amounts of the compound. The experiments were executed at room temperature and the measurements are devised in a plot $(\eta/\eta_0)^{1/3}$ *versus* r, where η = the viscosity of DNA in the presence of the compound, and η_0 = the viscosity of neat DNA in buffer solution.

EB–displacement studies: In order to determine and confirm the DNA–binding mode of the compound, a competitive study with EB as an intercalating marker is performed by fluorescence emission spectroscopy. Therefore, the EB–displacing ability of the compound from its EB–DNA conjugate was examined. The DNA–EB adduct was prepared by addition of 20 μM EB and 26 μM CT DNA in buffer solution (150 mM NaCl and 15 mM trisodium citrate at pH 7.0). The potential intercalation of the compound in-between the DNA–bases was studied by the addition of a certain amount of the compound solution into the EB–DNA

adduct solution. The influence of the compounds on the EB–DNA solution was monitored through the changes of the fluorescence emission spectra at excitation wavelength (λ_{ex}) at 540 nm.[S2] The tested compound does not show any significant fluorescence at room temperature in solution or in the presence of DNA, under the same experimental conditions (λ_{ex} = 540 nm). Bearing that in mind, the observed quenching of the EB–DNA solution is evidently associated to the displacement of EB from its EB–DNA adduct. The quenching efficiency (K_{SV}, in M^{-1}) for the compound was assessed according to the Stern–Volmer equation (eq. S2)[S2]:

$$\frac{Io}{I} = 1 + k_q \tau_0 [Q] = 1 + K_{SV}[Q] \qquad \text{(eq. S2)}$$

where I_0 and I = the fluorescence emission intensities of EB–DNA in the absence and presence of the quencher, respectively, [Q] = the concentration of the quencher (i.e. compound). K_{SV} is obtained from the Stern–Volmer plots by the slope of the diagram I_0/I *versus* [Q]. Taking τ_0 = 23 ns as the fluorescence lifetime of the EB–DNA system,[S3] the EB–DNA quenching constants (k_q, in $M^{-1}s^{-1}$) of the compound can be determined according to equation S4:

$K_{SV} = k_q \tau_o$ (eq. S3)

Interaction with serum albumins

The albumin–binding study for **1@NAP** was carried out by fluorescence emission quenching experiments using BSA (3 μM) or HSA (3 μM) in buffer solution (15 mM trisodium citrate and 150 mM NaCl at pH 7.0). The tested compound was used as quencher with gradually increasing concentrations to monitor the quenching of the emission intensity of tryptophan residues of BSA or HSA at 340-350 nm.[S2] The fluorescence emission spectra were recorded between 300–500 nm with excitation wavelength of 295 nm. All the experiments were conducted at room temperature.

The extent of the inner–filter effect can be roughly estimated with the following formula:

$$I_{corr} = I_{meas} \times 10^{\frac{\varepsilon(\lambda_{exc})cd}{2}} \times 10^{\frac{\varepsilon(\lambda_{em})cd}{2}} \qquad \text{(eq. S4)}$$

where I_{corr}= corrected intensity, I_{meas}= the measured intensity, c = the concentration of the quencher, d = the cuvette length (1 cm), $\varepsilon(\lambda_{exc})$ and $\varepsilon(\lambda_{em})$ = the ε of the quencher at the

excitation and the emission wavelength, respectively, as calculated from the UV–vis spectra of the compound.[S4]

The interaction of the quencher (i.e. compound **1**) with serum albumins was studied through the Stern–Volmer and Scatchard equations[S2] and corresponding graphs. The values of the respective Stern–Volmer constant K_{SV} (in M^{-1}), the quenching constant k_q (in $M^{-1}s^{-1}$), the SA–binding constant K (M^{-1}) and the number of binding sites per albumin (n) were calculated.

According to Stern–Volmer quenching equation[S2] (eq. S2), where I_0 = the initial tryptophan fluorescence intensity of SA, I = the tryptophan fluorescence intensity of SA after the addition of the quencher, k_q = the quenching rate constants of SA, K_{SV} = the dynamic quenching constant, τ_0 = the average lifetime of SA without the quencher, [Q] = the concentration of the quencher), the Stern–Volmer constant (K_{SV}, M^{-1}) can be obtained by the slope of the diagram I_0/I *versus* [Q]. Taking $\tau_0 = 10^{-8}$ s as fluorescence lifetime of tryptophan in SA,[S2] the quenching constant (k_q, $M^{-1}s^{-1}$) is calculated from equation S3.

From the Scatchard equation (eq. S5)[S2]:

$$\frac{\Delta I / I_0}{[Q]} = nK - K\frac{\Delta I}{I_0} \qquad \text{(eq. S5)}$$

where n = the number of binding sites per albumin and K = the SA–binding constant. The K constant (M^{-1}) is calculated from the slope in plots $(\Delta I/I_0)/[Q]$ *versus* $(\Delta I/I_0)$ and n is given by the ratio of y intercept to the slope.[S5]

References

[S1] A. Wolfe, G. Shimer and T. Meehan, *Biochemistry*, 1987, **26**, 6392.

[S2] J. R. Lakowicz, Principles of Fluorescence Spectroscopy, 3rd ed. Plenum Press, New York, 2006.

[S3] D. P. Heller and C. L. Greenstock, *Biophys. Chem.*, 1994, **50**, 305.

[S4] L. Stella, A. L. Capodilupo and M. Bietti, *Chem. Commun.*, 2008, 4744.

[S5] Y. Wang, H. Zhang, G. Zhang, W. Tao and S. Tang, *J. Lumin.*, 2007, **126**, 211.

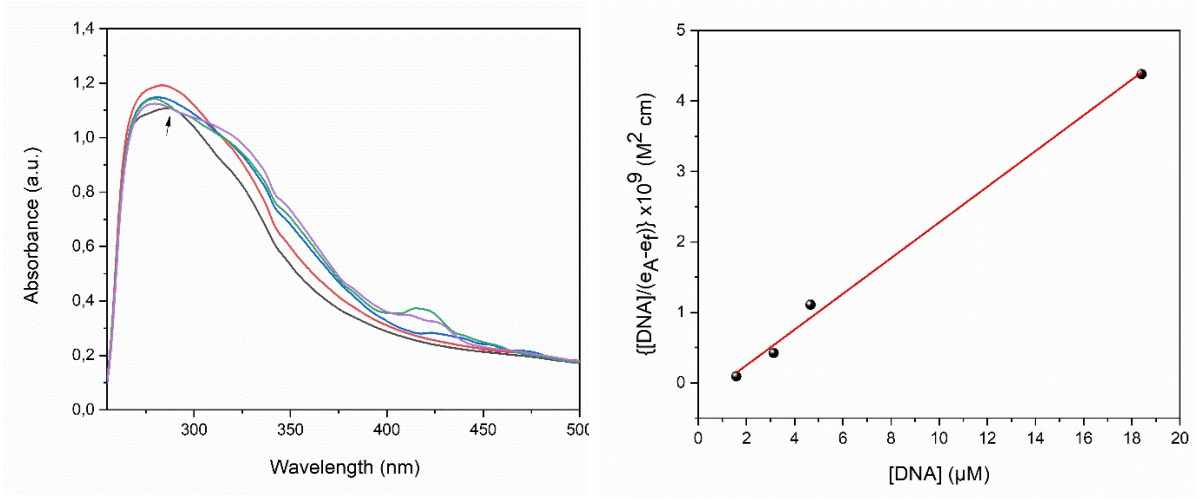

(A) **(B)**

Fig. S10. (A) UV–vis spectra of DMSO solution of compound **1@NAP** in the presence of increasing amounts of CT DNA. The arrow shows the changes upon addition of increasing amounts of CT DNA. (B) Plot of $\frac{[DNA]}{(\varepsilon_A - \varepsilon_f)}$ *versus* [DNA] for compound **1@NAP.**

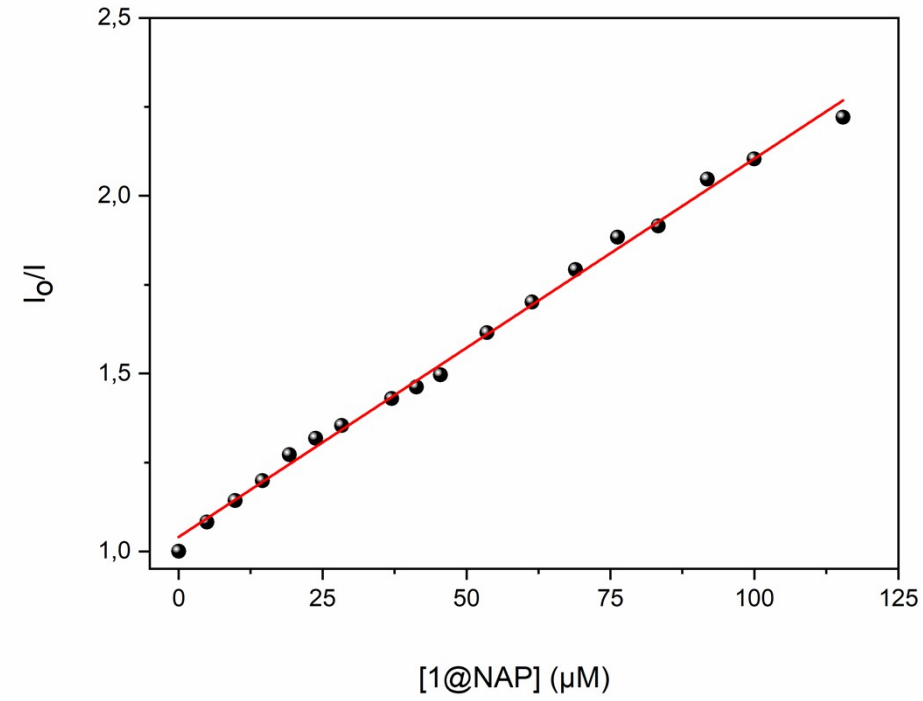

Fig. S11. Stern–Volmer quenching plot of EB bound to CT DNA for compound **1@NAP.**

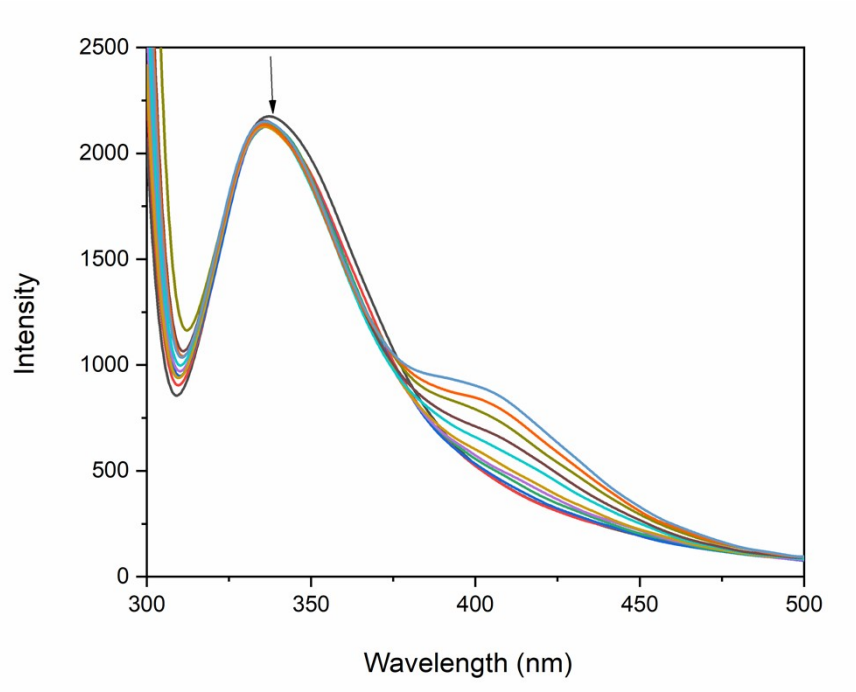

Fig. S12. Fluorescence emission spectra ($\lambda_{excitation}$ = 295 nm) for HSA (3 µM) in buffer solution (150 mM NaCl and 15 mM trisodium citrate at pH 7.0) upon addition of increasing amounts of compound **1@NAP**. The arrow shows the changes of intensity upon increasing amounts of the compound**.**

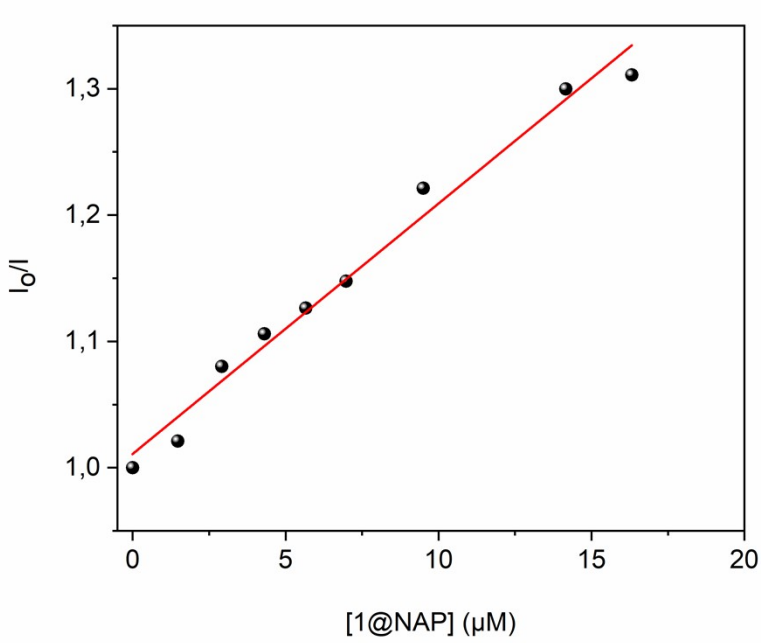

Fig. S13. Stern–Volmer quenching plot of BSA for compound **1@NAP**.

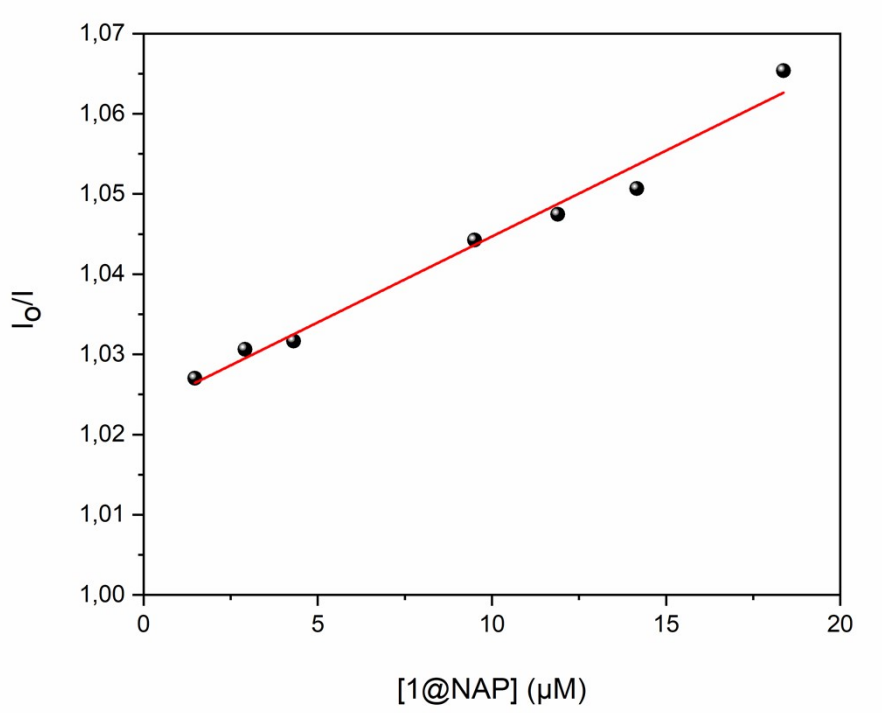

Fig. S14. Stern–Volmer quenching plot of HSA for compound **1@NAP**.

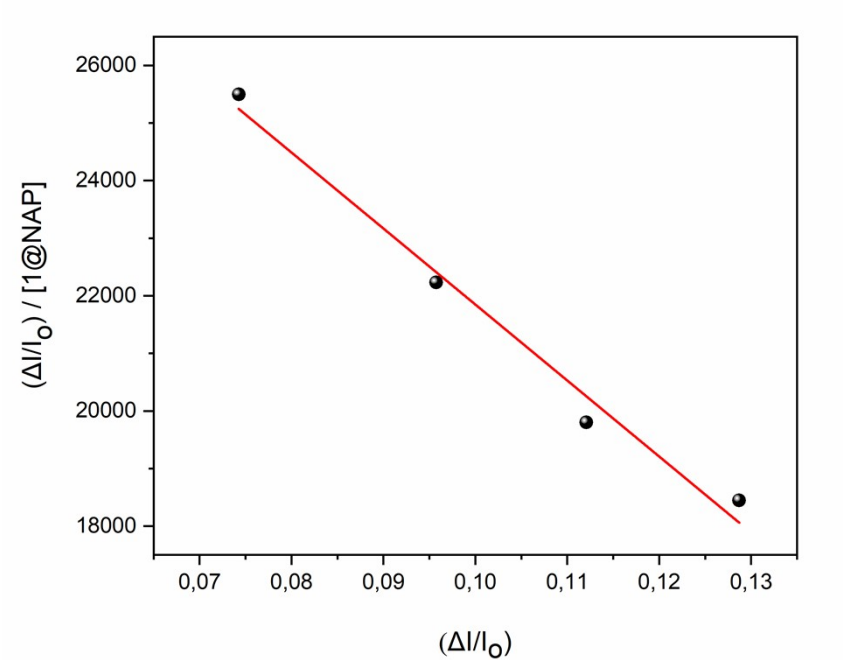

Fig. S15. Scatchard plot of BSA for compound **1@NAP**.

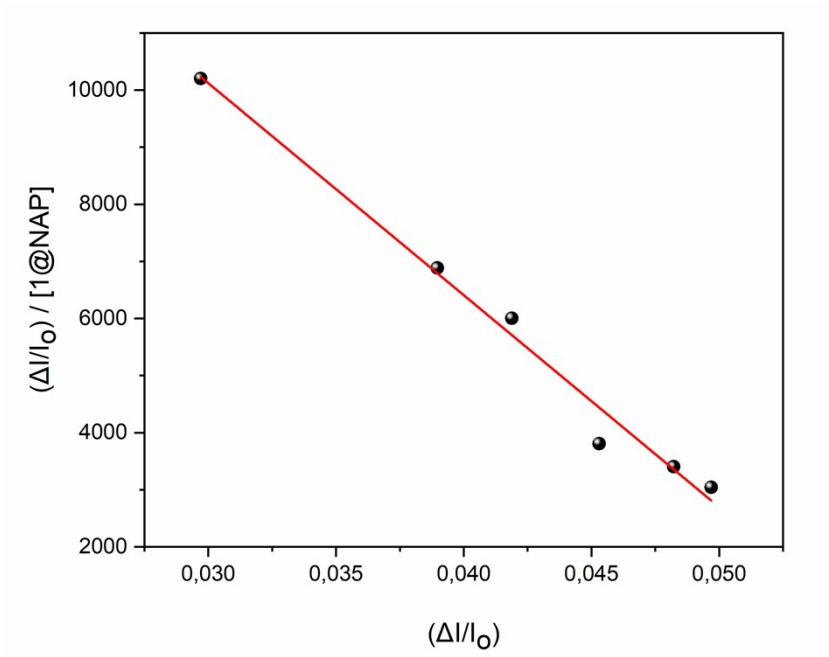

Fig. S16. Scatchard plot of HSA for compound **1@NAP**.